Magnetism in Solids

Magnetic Phase Transition of $La_{1-x}Sr_xMnO_3$ Induced by Charge Transfer and Interdiffusion

Angus Huang[1], Ching-Hao Chang[2], and Horng-Tay Jeng[1,3]

[1]*Department of Physics, National Tsing Hua University, Hsinchu 30013, Taiwan*
[2]*Institute for Theoretical Solid State Physics, IFW Dresden, Dresden 01069, Germany*
[3]*Institute of Physics, Academia Sinica, Taipei 11529, Taiwan*

Received 19 Aug 2016, revised 4 Nov 2016, accepted 15 Nov 2016, published 24 Nov 2016, current version 8 Feb 2017.

Abstract—Rare earth manganites under hole doping, $R_{1-x}B_xMnO_3$ (R = La, Nd, Pr and B = Sr, Ca, Ba), have a rich charge carrier-temperature-magnetism phase diagram. The phases are tunable by applying external constraints, such as strain and boundary conditions. For example, the ferromagnetic phase dominated by the double-exchange mechanism can be transformed into an antiferromagnetic phase by controlling the doping level. In this work, using first principles calculations based on density functional theory, we study the bilayer system $La_{0.67}Sr_{0.33}MnO_3$ (LSMO)/$SrRuO_3$ (SRO) composed of two ferromagnetic materials. The original ferromagnetism in LSMO becomes A-type antiferromagnetism at the interface. Such intriguing behavior at transition-metal oxide interfaces in the LSMO/SRO bilayer, stemming from coexisting interdiffusion and charge transfer from the SRO layer, is similar to a hole-doped LSMO layer attached to a substrate with electric polarization. Our result qualitatively and quantitatively explains recent experimental evidence of a dramatic change in the strength of magnetization for different terminations of LSMO/SRO bilayers.

Index Terms—Magnetism in solids, electrical control of spin, magneto-electric materials, magnetic films, magnetic oxides.

I. INTRODUCTION

The strong correlation of localized d electrons plays the key role in transition metal oxides (TMO) and exhibits many fascinating properties, including magnetism [Tokura 2000], superconductivity [Takahashi 2008], ferroelectricity [van den Brink 2008], orbital or charge ordering [Murakami 1998] and charge transfer [Basletic 2008]. In the perovskite structure, the six oxygen ions surrounding the cation generate the octahedral crystal field and split the fivefold degenerate d orbitals of the cations into t_{2g} and e_g states, which originates additional degree of freedom and leads to many complex quantum phases. For example, strontium doped lanthanum manganite, $La_{1-x}Sr_xMnO_3$ (LSMO), is famous as its rich magnetic phasediagram relative to the strontium concentration, strain and temperature [Tokura 2000]. Depending on different occupations in the t_{2g} and e_g orbitals, the Mn cations can lead to superexchange or double exchange mechanism. The competitions between the strain and doping effects result in the complicated phases.

In particular, the TMO heterostructures have attracted a lot of investigations in recent years because the emergent interfacial states may present novel properties different from those in the original bulk phases. A famous system is $LaAlO_3$/$SrTiO_3$ (LAO/STO) bilayer oxide. Both of the LAO and STO are insulators with a large band gap but the interface of the heterostructure shows a high mobility two dimensional electron gas (2DEG) owing to the charge transfer [Ohtomo 2003], and this 2DEG further turns into a superconductor at low temperature [Reyren 2007]. Experimental and theoretical studies demonstrate new type magnetisms in the emergent interfacial states in bilayer systems such as $BaTiO_3$/LSMO [Burton 2009, Lu 2012, Chen 2014], $PbZr_xTi_{1-x}O_3$ (PZT)/LSMO [Kumar 2015], $PbTiO_3$/LSMO [Chen 2012] and $BiFeO_3$/LSMO [Yu 2010]. The above heterostructures are all composed by a piezoelectric or ferroelectric layer with another LSMO layer. The magnetic phases of the latter are sensitive to the structure, orbital or charge ordering. By modulating the interfacial conditions via applying strain or changing termination, the structure of the interface can be distorted, and the electrons may accumulate or deplete such that a magnetic phase transition occurs at the interface of LSMO. The latter magnetic phase transition implies the possibility of tuning the magnetic ordering by electric fields, which is called magnetoelectric effects.

The $La_{1-x}Sr_xMnO_3$/$SrRuO_3$ (LSMO/SRO) bilayer system with $x \sim 0.33$ has been experimentally studied recently [Ziese 2012, Ke 2013, Das 2015, 2016]. Both the buck LSMO and SRO are ferromagnetic with Curie temperature of 300 K and 150 K, respectively [Hemberger 2002, Koster 2012]. When these two materials are stacked into the bilayer system, the magnetism–temperature curves demonstrate two different magnetic phase transition temperatures at 300 K and 150 K, which are similar to their bulk Curie temperatures. Moreover, in the cooling process, the total magnetism increases at 300 K and decreases at 150 K [Ziese 2012, Das 2016]. These two characteristics indicate that the main contributions of the magnetic order of LSMO and SRO are still ferromagnetism. Furthermore, the decrease of total magnetic moments at 150 K imply that the spin directions of the two oxides are antiparallel in the bilayer system [Ziese 2012, Das 2016]. However, when the stacking method is different, the total magnetism at low temperature will change even if the sample is cooling in strong magnetic field [Das 2016]. This implies the magnetic phase transition in bilayer system is actually dependent on the layer stacking.

In this work, we study the interfacial emergent state in LSMO/SRO system by using first principles calculations and present the relations among the magnetic phase, interfacial diffusion, and charge transfer.

Corresponding authors: C.-H. Chang (cutygo@gmail.com) and H.-T. Jeng (jeng@phys.nthu.edu.tw).
Digital Object Identifier 10.1109/LMAG.2016.2633060

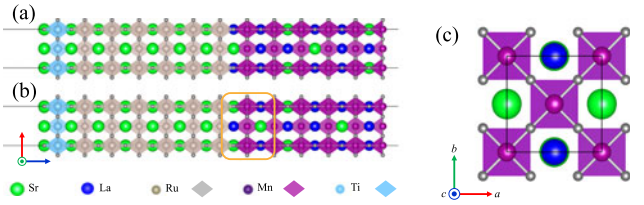

Fig. 1. The supercell (s.c.) structure of LSMO/SRO negative type (N-type) used in calculation. The diamond icons mean the octahedral of the MO_6, M = Ru, Mn, Ti. (a) Homogeneous case, including 6 unit cell (u.c.) LSMO, 6 u.c. SRO and 1 u.c. STO, here 1 u.c. STO is substrate and LSMO is covering SRO with $La_{0.5}Sr_{0.5}O$ middle layer. The surface is cutting in MnO atomic layer that is similar to perovskite growing conditions. (b) Non-homogeneous case, has similar architecture with above one, whereas the doping of Sr $\sim$ 0.5 in the orange region. (c) Top view of N-type homogeneous case. Each layer of unit cell center in cations and contains two oxide octahedral without distortion.

We further compare the results with previous experimental studies. We demonstrate that both interfacial diffusion and charge transfer in LSMO/SRO bilayer participate the magnetic phase transition at the interface.

II. METHOD

We perform *ab initio* calculations based on the density functional theory (DFT) framework by using the VASP package. The projector augmented wave method (PAW) and LSDA+U exchange-correlated energies are utilized. For the present calculations, Ti $3d^3 4s^1$, La $5s^2 5p^6 5d^1 6s^2$, Sr $4s^2 4p^6 5s^2$, Mn $3d^6 4s^1$, Ru $4d^7 5s^1$, O $2s^2 2p^4$ are considered as the valance electrons. The energy cutoff is 400 eV and the k-point mesh used is $8 \times 8 \times 1$ containing the Γ point and zone boundaries. We have carefully examined the total energy convergence upon the number of plane waves and k points. The vacuum thickness larger than 15 Å is used in our calculations. The on-site Coulomb repulsion $U = 3.5$ eV for Ru d orbitals [Jeng 2006], $U = 3.0$ eV for Mn d orbitals [Colizzi 2007] and $U = 6.0$ eV for La f orbitals are used in LSDA+U calculations. For simplicity, we use the simple cubic structure and do not consider the minor JT effect or lattice distortions. The lattice parameter used for the LSMO/SRO heterostructure is 3.88 Å which is the same as the average a, b of geometrically optimized SRO. The resultant ignorable lattice mismatch with the LSMO lattice parameters is less than 1%. We used the $\sqrt{2} \times \sqrt{2}$ supercell for studying the doping effect of Sr ions in LSMO crystal. Moreover, the self-consistent process is calculated until the total energy conserve to 10^{-6} eV.

III. RESULT

A. N-Type LSMO/SRO Bilayer System

Firstly, we consider the bilayer system LSMO on top of the SRO within the $\sqrt{2} \times \sqrt{2}$ supercell. Both LSMO and SRO are 6 unit cell (u.c.) thick along the z direction with one u.c. $SrTiO_3$ (STO) as the substrate [see Fig. 1(a)]. The LSMO layer is terminated with MnO_2. Due to the limit of crystal growing methods, this stacking has the interface LaO/RuO_2 between LSMO and SRO layers. To simulate the doping effect of Sr ions, there are 4 La ions and 2 Sr ions occupying 3 LSMO layers.

With this stacking, the LSMO/SRO interface accumulates the electrons to balance the charge in the heterostructure. In fact, this phenomenon is the same as that in the LAO/STO two dimensional electron gas (LAO/STO 2D EG). In these bilayer systems, one of them such as $La_{1-x}Sr_xMnO_3$ contains non-neutral layers $\left(La^{3+}_{0.67}Sr^{2+}_{0.33}O^{2-}\right)^{0.67}$ or $\left(Mn^{3.33+}\left(O^{2-}\right)_2\right)^{0.67-}$, while the other consists of charge-neutral layers. The cutting face of non-neutral layers causes the polar catastrophe that the electric potential diverges [Nakagawa 2006]. To avoid this the charge transfer occurs and screens out the electric potential, thus electrons accumulate at the interface. We name it the negative-type bilayer system (N-type) for these electron-collecting interfaces. We calculate the magnetism of LSMO and SRO with parallel (MP) and anti-parallel (AP) spin arrangements. The calculated total energies of AP are lower than those of MP by 4.3 meV (see Table 1). This effect can be understood as the superexchange between the SRO and LSMO according to the Goodenough–Kanamori–Anderson rules (GKA rules) [Opel 2012]. The fully occupation of Mn majority t_{2g} and Ru minority t_{2g} d orbital exhibits virtual hopping when they are antiparallel, and the Mn e_g orbital can also hop to Ru e_g orbital and give a weak parallel magnetism. Therefore, the total effect of hopping leads to parallel magnetism at the interface. The calculated results are similar to the previous experiments.

TABLE 1. The total energy E (meV/s.c.) and total magnetic moment M (μ_B/s.c.) of LSMO/SRO bilayer systems from DFT result with different structures and magnetic phases. The energies of N-type non-homo structure with A-type magnetic phase (N non-homo A) as the zero. All the values in the table are averaged such that each layer in the supercell only including one magnetic cations.

	Spin ordering LSMO/SRO	Energy (meV/s.c.)	Moment (μ_B/s.c.)
N non-homo AP	↑↑↑↑↑↑ / ↓	553.8	10.22
N non-homo A	↑↑↑↑↑↓ / ↓	0.0	2.96
N non-homo A2	↑↑↑↑↓↓ / ↓	3.8	−4.30
N non-homo A3	↑↑↑↑↓↑ / ↓	28.5	3.04
N homo AP	↑↑↑↑↑↑ / ↓	260.1	10.26
N homo MP	↓↓↓↓↓↓ / ↓	264.4	−33.94
P non-homo AP	↑↑↑↑↑↑ / ↓	872.2	8.70
P homo AP	↑↑↑↑↑↑ / ↓	426.9	9.45
P homo MP	↓↓↓↓↓↓ / ↓	437.0	−35.25

However, the charge transfer is not the only degree of freedom in LSMO/SRO bilayer system. Similar to LAO/STO bilayer system, the charge transfer accumulates delocalized electrons and increases the interface dipole energies. Therefore, the Sr and La ions cross over the interface to compensate the dipoles [Nakagawa 2006, Hwang 2012]. To consider the Sr ion interdiffusion, we calculate the N-type non-homogenous (N-type non-homo) [see Fig. 1(b)]. That is, we move positions of Sr and La ions in LSMO such that the two layers' non-magnetic cations near SRO are La_2Sr_2 (doping $x = 0.5$). On the other hand, the other four layers are La_6Sr_2 (doping $x = 0.25$). Because of the metallic nature of LSMO with strong screening effect, the interdiffusion only occurs within one to two layers [Lüth 2015]. It is worth noting that we keep the total number of each kind of atoms the same in homo and non-homo systems so that the total energies given from DFT would be comparable. To determine the magnetic ground state of N-type homo and N-type non-homo cases, we performed calculations for different magnetic orientations in LSMO around the interface as listed in Table 1, including ferromagnetism, A-type and C-type antiferromagnetism. The calculated results of various magnetic configurations are given below.

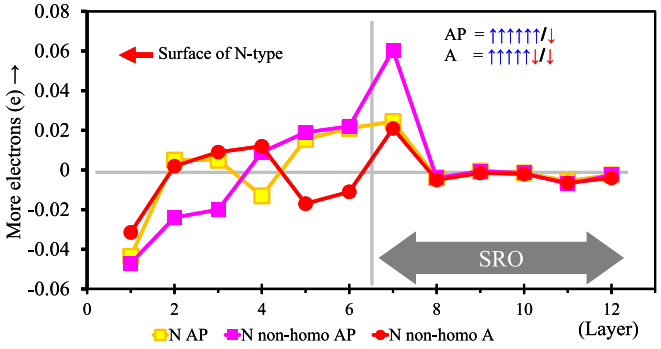

Fig. 2. From the results of first principle, plotting charge distributions of Mn/Ru in LSMO/SRO N-type structure layer by layer, surface of the system numbered with 1. The zero points of charges in the left/right part use the average charges of Mn/Ru ions, and all the situations the interfaces attract elections in the SRO sides. In the system N-type non-homogenous with magnetism type A, there is an obvious charge variance at the interface.

For the N-type non-homo case shown in Table 1, the highest total energy of the LSMO/SRO bilayer is given from the ferromagnetic LSMO layer. With the magnetic moments of LSMO flipped around the interface, the total energy of the bilayer is lowered down because the LSMO is relatively closer to the AFM phase (see the phase diagram in Fig. 6 of Chmaissem [2003]) in the N-type non-homo case with a higher Sr density. Moreover, these structures and magnetic phases are relatively stable compared to other N-type homo or N-type non-homo magnetic phases, indicating that the A phase would be the ground state in the presence of the interdiffusion in the N-type LSMO/SRO bilayer system.

To clarify the magnetic phase transition and the charge of magnetic cations, we studied the charge modulation with different magnetic states and structures. In Fig. 2 we present the layer-resolved charge distributions including the N AP, N non-homo A and N non-homo AP systems. As can be seen, the N-type interface always accumulates electrons as discovered in previous studies. Moreover, the N-type non-homo case with antiparallel magnetism causes a non-saturated charge gradient, which implies it is unstable. The charge gradient can be removed by turning the emergent interface state into magnetic A phase, which indicates this magnetic phase transition is strongly coupled to the electric properties.

The removable charge gradient is similar to the tunable electron accumulation at the interface in the LSMO/ferroelectric bilayer system. The charge transfers at the N-type LSMO/SRO bilayer interface originate an effective electric potential similar to the ferroelectric materials and modulate the magnetic ordering at the interface, even though both the LSMO and SRO are metallic and non-ferroelectric which strongly differs from the $BaTiO_3$/LSMO system.

B. P-Type Bilayer System and Electronic Structure

In Section III-A, we showed that the N-type LSMO/SRO bilayer system exhibits a magnetic phase transition due to the Sr interdiffusion. However, the interdiffusion is not the unique condition of the interfacial magnetic reconstruction. Here we also consider the positive-type bilayer system (P-type bilayer system) in the LSMO/SRO bilayer [see Fig. 3(a)]. Similar to LAO/STO bilayer systems, the main structure difference between the N-type and the P-type is that the N-type interface terminates at LaO/RuO_2 layer and the P-type one terminates at

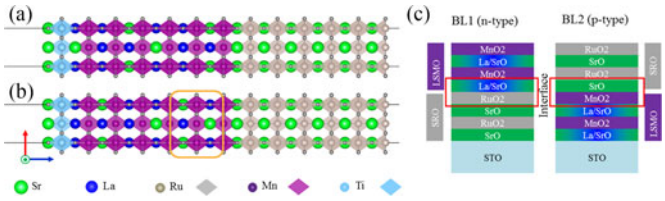

Fig. 3. The structures of positive-type LSMO/SRO bilayer system (P-type). (a), (b) homogeneous and non-homogeneous cases of P-type LSMO/SRO. The LSMO and SRO are medium with SrO atomic layer. The surfaces of the systems are terminal with RuO layer. (c) Comparison of N-type and P-type structure.

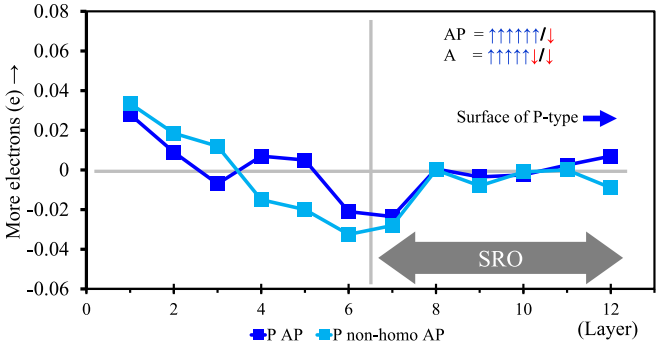

Fig. 4. Charge distributions of magnetic cations in LSMO/SRO P-type systems, including homogenous and non-homogeneous cases. Both of cases are loss electrons in LSMO/SRO interfaces. Again, the zero points of charge in the left and right parts use the average charges of Mn and Ru ions, respectively.

SrO/MnO_2 layer [see Fig. 3(c)]. Due to the non-charge-neutral layer in LSMO, the electrons accumulate at the N-type bilayer interface, in contrast to holes accumulate at the P-type interface. Furthermore, it is easier for ions to interdiffuse at the N-type than at the P-type interface since the P-type interface is much sharper due to the lack of delocalized screening electrons or hole charges at the P-type interface [Nakagawa 2006]. Similar to the N-type cases, we also calculate many different magnetic phases for the P-type homo and non-homo structures as shown in Table 1. Like the N-type structure, both the non-homo and homo cases have the same number of La and Sr ions. We then exchange the La and Sr ions to simulate the interdiffusion. We find that the main contributions of magnetism from LSMO and SRO are still anti-parallel. The P-type homo bilayer system with anti-parallel magnetism (P-type AP) are stabler than the parallel magnetism (P-type MP) by 10.1 meV per supercell. However, even if the P-type case has same degree of Sr interdiffusion with the N-type case, the ground state of LSMO is still ferromagnetic, which indicates that both electric and structural effects are important to the interface magnetic phase transition. We also study the charge distribution of the P-type systems (see Fig. 4). Both the P-type homo AP and P-type non-homo AP accumulate holes at the interface while the charge distributions of the homo structure are smoother. These results agree with the discussion above.

Finally, we show that the change of magnetic phases leads to a significant change in electronic structures. SRO is a minority-band itinerant ferromagnet, namely the spin down band appears at the Fermi level while the total magnetization of SRO is spin up because of the fully occupied t_{2g} ↑ band and partially filled t_{2g} ↓ band. We consider a $La_{0.67}Sr_{0.33}MnO_3$ layer with magnetization opposite to that of SRO layer. As these two layers are combined to form a LSMO/SRO bilayer with anti-parallel (AP) spin arrangement, the majority carriers

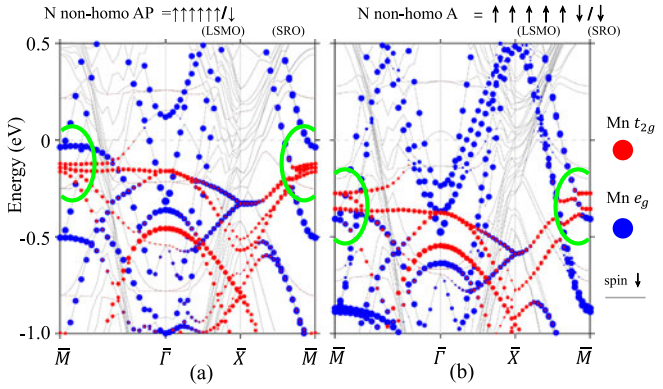

Fig. 5. The band structures of N-type LSMO/SRO bilayers with (a) non-homo AP and (b) non-homo A phases. Here the red (blue) points indicate the components of Mn t_{2g} (e_g) orbitals with spin antiparallel to the SRO magnetization.

(e_g electrons) of LSMO layer can enter and interact with SRO layer because the spin is antiparallel to the SRO magnetization. Such interaction with the higher SRO minority bands leads the majority bands of LSMO close to the Fermi level [see blue and red flat bands near zero energy around the M point in Fig. 5(a)]. While in the A magnetic phase, the interaction between LSMO majority carriers and SRO layer is at a relatively lower energy due to interactions with the lower SRO majority bands. Therefore, the bands near Fermi level in AP phase are moved apart from Fermi level in A phase [see blue and red flat bands around the M point in Fig. 5(b)]. The change between AP and A magnetic structures indeed leads to a dramatic change of electronic structures, which can largely impact the transport and other related physical properties in LSMO/SRO bilayer. Therefore, the carrier density and transport property are sensitive to the switch of magnetic phases, since the phase decides the electronic structure at Fermi level.

IV. DISCUSSIONS AND CONCLUSIONS

As a MnO_2 layer in LSMO flips its magnetization to the opposite direction, it reduces the magnetization by $3.7 \times 2 \approx 7\ \mu_B$ for a Mn^{4+} atom has a moment of $3.7\ \mu_B$. This explains why the magnetization difference between the N-type non-homo A and P-type homo A is approximately $6.5\ \mu_B$ (see Table 1). A recent experiment has observed that the magnetization in the N-type system is much lower than that of the P-type one (see Fig. 3 in Das [2016], where the termination 1 (2) refers to our P-type (N-type) system). The measured magnetization difference per unit cell between two systems is approximately $0.7 \times 9 \approx 6.3\ \mu_B$, where $0.7\ \mu_B$ is the averaged magnetization difference per MnO_2 layer and 9 is the amount of total LSMO layers (see [Das 2016]). Therefore, our results not only qualitatively explain why N-type has lower magnetization, but also obtain a value of magnetization difference ($6.5\ \mu_B$), which is almost the same with the measured ($6.3\ \mu_B$).

The difference between our result and previous studies of magnetoelectric effects is that previous studies utilize the ferromagnetism materials to control the d orbital occupation in Mn or to tune the strain to control the populations of t_{2g} orbitals so as to influence the magnetic phase, while in this work we show that in LSMO/SRO N-type non-homogenous case, the magnetic ground state can be influenced by charge accumulation. It opens up a new way to study the coupling between magnetic properties and electric properties, and can potentially be applied to magnetic tunneling junctions.

To summarize, by using the *ab initio* density functional calculations, we have studied several phases of LSMO/SRO bilayer systems to clarify the magnetic ground state. We show that the SRO and LSMO prefer anti-parallel spins in bilayer system. The P-type bilayer shows no magnetic phase transition even considering the interdiffusion effect. While in N-type LSMO/SRO, the ionic interdiffusion and charge transfer coexist, matching the experimental findings that the magnetic ground state of LSMO turn from ferromagnetic into A-type antiferromagnetic at the interface. We also prove, by simulating the P-type bilayer system with the same degree of ion-interdiffusion, that this effect is based on the coexistence of the charge transfer and interdiffusion, which agrees with recent experiments [Das 2016].

ACKNOWLEDGMENT

The authors thank S. Das, T.-R. Chang, H. Lee, and P.-J. Chen for helpful discussions. This work was supported by NCTS, Ministry of Science and Technology, Academia Sinica, and National Tsing Hua University, Taiwan.

REFERENCES

Basletic M, Maurice J-L, Carrétéro C, Herranz G, Copie O, Bibes M, Jacquet É, Bouzehouane K, Fusil S, Barthélémy A (2008), "Mapping the spatial distribution of charge carriers in $LaAlO_3/SrTiO_3$ heterostructures," *Nature Mater.*, vol. 7, pp. 621–625, doi: 10.1038/nmat2223.

Burton J D, Tsymbal E Y (2009), "Prediction of electrically induced magnetic reconstruction at the manganite/ferroelectric interface," *Phys. Rev. B*, vol. 80, 174406, doi: 10.1103/PhysRevB.80.174406.

Chen H, Ismail-Beigi S (2012), "Ferroelectric control of magnetization in $La_{1-x}Sr_xMnO_3$ manganites: A first-principles study," *Phys. Rev. B*, vol. 86, 024433, doi: 10.1103/PhysRevB.86.024433.

Chen H, Qiao Q, Marshall M S J, Georgescu A B, Gulec A, Phillips P J, Klie R F, Walker F J, Ahn C H, Ismail-Beigi S (2014), "Reversible modulation of orbital occupations via an interface-induced polar state in metallic manganites," *Nano Lett.*, vol. 14, pp. 4965–4970, doi: 10.1021/nl501209p.

Chmaissem O, Dabrowski B, Kolesnik S, Mais J, Jorgensen J D, Short S (2003), "Structural and magnetic phase diagrams of $La_{1-x}Sr_xMnO_3$ and $Pr_{1-y}Sr_yMnO_3$," *Phys. Rev. B*, vol. 67, 094431, doi: 10.1103/PhysRevB.67.094431.

Colizzi G, Filippetti A, Fiorentini V (2007), "Magnetism of $La_{0.625}Sr_{0.375}MnO_3$ under high pressure from first principles," *Phys. Rev. B*, vol. 76, 064428, doi: 10.1103/PhysRevB.76.064428.

Das S, Herklotz A, Pippel E, Guo E J, Rata D, Dörr K (2015), "Strain dependence of antiferromagnetic interface coupling in $La_{0.7}Sr_{0.3}MnO_3/SrRuO_3$ superlattices," *Phys. Rev. B*, vol. 91, 134405, doi: 10.1103/PhysRevB.91.134405.

Das S, Rata A D, Maznichenko I V, Agrestini S, Pippel E, Chen K, Valvidares S M, Babu V H, Herrero-Martin J, Pellegrin E, Nenkov K, Herklotz A, Ernst A, Mertig I, Hu Z, Dörr K (2016), "Termination control of magnetic coupling at a complex oxide interface," preprint, https://arxiv.org/abs/1606.08687.

Hemberger J, Krimmel A, Kurz T, von Nidda H-A K, Ivanov V Y, Mukhin A A, Balbashov A M, Loidl A (2002), "Structural, magnetic, and electrical properties of single-crystalline $La_{1-x}Sr_xMnO_3$ ($0.4 < x < 0.85$)," *Phys. Rev. B*, vol. 66, 094410, doi: 10.1103/PhysRevB.66.094410.

Hwang H Y, Iwasa Y, Kawasaki M, Keimer B, Nagaosa N, Tokura Y (2012), "Emergent phenomena at oxide interfaces," *Nature Mater.*, vol. 11, pp. 103–113, doi: 10.1038/nmat3223.

Jeng H-T, Lin S-H, Hsue C-S (2006), "Orbital ordering and Jahn-Teller distortion in perovskite ruthenate $SrRuO_3$," *Phys. Rev. Lett.*, vol. 97, 067002, doi: 10.1103/PhysRevLett.97.067002.

Ke X, Belenky L J, Lauter V, Ambaye H, Bark C W, Eom C B, Rzchowski M S (2013), "Spin structure in an interfacially coupled epitaxial ferromagnetic oxide heterostructure," *Phys. Rev. Lett.*, vol. 110, 237201, doi: 10.1103/PhysRevLett.110.237201.

Koster G, Klein L, Siemons W, Rijnders G, Dodge J S, Eom C-B, Blank D H A, Beasley M R (2012), "Structure, physical properties, and applications of $SrRuO_3$ thin films," *Rev. Mod. Phys.*, vol. 84, pp. 253–298, doi: 10.1103/RevModPhys.84.253.

Kumar A, Barrionuevo D, Ortega N, Shukla A K, Shannigrahi S, Scott J F, Katiyar R S (2015), "Ferroelectric capped magnetization in multiferroic PZT/LSMO tunnel junctions," *Appl. Phys. Lett.*, vol. 106, 132901, doi: 10.1063/1.4916732.

Lu H, George T A, Wang Y, Ketsman I, Burton J D, Bark C W, Ryu S, Kim D J, Wang J, Binek C, Dowben P A, Sokolov A, Eom C B, Tsymbal E Y, Gruverman A (2012), "Electric modulation of magnetization at the $BaTiO_3/La_{0.67}Sr_{0.33}MnO_3$ interfaces," *Appl. Phys. Lett.*, vol. 100, 232904, doi: 10.1063/1.4726427.

Lüth H (2015), *Solid Surfaces, Interfaces and Thin Films*, 6th ed., New York, NY, USA: Springer, pp. 395.

Murakami Y, Kawada H, Kawata H, Tanaka M, Arima T, Moritomo Y, Tokura Y (1998), "Direct observation of charge and orbital ordering in $La_{0.5}Sr_{1.5}MnO_4$," *Phys. Rev. Lett.*, vol. 80, pp. 1932–1935, doi: 10.1103/PhysRevLett.80.1932.

Nakagawa N, Hwang H Y, Muller D A (2006), "Why some interfaces cannot be sharp," *Nature Mater.*, vol. 5, pp. 204–209, doi: 10.1038/nmat1569.

Ohtomo A, Hwang H Y (2004), "A high-mobility electron gas at the $LaAlO_3/SrTiO_3$ heterointerface," *Nature*, vol. 427, pp. 423–426, doi: 10.1038/nature02308.

Opel M (2012), "Spintronic oxides grown by laser-MBE," *J. Phys. D: Appl. Phys.*, vol. 45, 033001, doi: 10.1088/0022-3727/45/3/033001.

Reyren N, Thiel S, Caviglia A D, Kourkoutis L F, Hammerl G, Richter C, Schneider C W, Kopp T, Rüetschi A-S, Jaccard D, Gabay M, Muller D A, Triscone J-M, Mannhart J (2007), "Superconducting interfaces between insulating oxides," *Science*, vol. 317, pp. 1196–1199, doi: 10.1126/science.1146006.

Takahashi H, Igawa K, Arii K, Kamihara Y, Hirano M, Hosono H (2008), "Superconductivity at 43 K in an iron-based layered compound $LaO_{1-x}F_xFeAs$," *Nature*, vol. 453, pp. 376–378, doi: 10.1038/nature06972.

Tokura Y, Nagaosa N (2000), "Orbital physics in transition-metal oxides," *Science*, vol. 288, pp. 462–468, doi: 10.1126/science.288.5465.462.

van den Brink J, Khomskii D I (2008), "Multiferroicity due to charge ordering," *J. Phys.: Condens. Matter*, vol. 20, 434217, doi: 10.1088/0953-8984/20/43/434217.

Yu P, Lee J-S, Okamoto S, Rossell M D, Huijben M, Yang C H, He Q, Zhang J X, Yang S Y, Lee M J, Ramasse Q M, Erni R, Chu Y-H, Arena D A, Kao C-C, Martin L W, Ramesh R (2010), "Interface ferromagnetism and orbital reconstruction in $BiFeO_3$-$La_{0.7}Sr_{0.3}MnO_3$ heterostructures," *Phys. Rev. Lett.*, vol. 105, 027201, doi: 10.1103/PhysRevLett.105.027201.

Ziese M, Bern F, Pippel E, Hesse D, Vrejoiu I (2012), "Stabilization of ferromagnetic order in $La_{0.7}Sr_{0.3}MnO_3$-$SrRuO_3$ superlattices," *Nano Lett.*, vol. 12, pp. 4276–4281, doi: 10.1021/nl301963a.